



Effect of Intensity and Mode of Artificial Upwelling on Particle Flux and Carbon Export

Moritz Baumann^{1*}, Jan Taucher¹, Allanah J. Paul¹, Malte Heinemann², Mari Vanharanta^{3,4}, Lennart T. Bach⁵, Kristian Spilling^{3,6}, Joaquin Ortiz¹, Javier Arístegui⁷, Nuzet Hernández-Hernández⁷, Isabel Baños⁷ and Ulf Riebesell¹

¹ Marine Biogeochemistry, Biological Oceanography, GEOMAR Helmholtz Centre for Ocean Research Kiel, Kiel, Germany, ² Institute of Geosciences, Kiel University, Kiel, Germany, ³ Marine Research Centre, Finnish Environment Institute, Helsinki, Finland, ⁴ Tvärminne Zoological Station, University of Helsinki, Hanko, Finland, ⁵ Institute for Marine and Antarctic Studies, University of Tasmania, Hobart, TAS, Australia, ⁶ Centre for Coastal Research, University of Agder, Kristiansand, Norway, ⁷ Oceanografía Biológica, Instituto de Oceanografía y Cambio Global, Universidad de Las Palmas de Gran Canaria, Las Palmas de Gran Canaria, Spain

OPEN ACCESS

Edited by:

Angelicque White,
University of Hawai'i at Mānoa,
United States

Reviewed by:

Chin-Chang Hung,
National Sun Yat-sen University,
Taiwan

Bieito Fernández Castro,
University of Southampton,
United Kingdom

*Correspondence:

Moritz Baumann
mbaumann@geomar.de

Specialty section:

This article was submitted to
Marine Biogeochemistry,
a section of the journal
Frontiers in Marine Science

Received: 15 July 2021

Accepted: 05 October 2021

Published: 27 October 2021

Citation:

Baumann M, Taucher J, Paul AJ, Heinemann M, Vanharanta M, Bach LT, Spilling K, Ortiz J, Arístegui J, Hernández-Hernández N, Baños I and Riebesell U (2021) Effect of Intensity and Mode of Artificial Upwelling on Particle Flux and Carbon Export. *Front. Mar. Sci.* 8:742142. doi: 10.3389/fmars.2021.742142

Reduction of anthropogenic CO₂ emissions alone will not sufficiently restrict global warming and enable the 1.5°C goal of the Paris agreement to be met. To effectively counteract climate change, measures to actively remove carbon dioxide from the atmosphere are required. Artificial upwelling has been proposed as one such carbon dioxide removal technique. By fueling primary productivity in the surface ocean with nutrient-rich deep water, it could potentially enhance downward fluxes of particulate organic carbon (POC) and carbon sequestration. In this study we investigated the effect of different intensities of artificial upwelling combined with two upwelling modes (recurring additions vs. one singular addition) on POC export, sinking matter stoichiometry and remineralization depth. We carried out a 39 day-long mesocosm experiment in the subtropical North Atlantic, where we fertilized oligotrophic surface waters with different amounts of deep water. The total nutrient inputs ranged from 1.6 to 11.0 μmol NO₃⁻ L⁻¹. We found that on the one hand POC export under artificial upwelling more than doubled, and the molar C:N ratios of sinking organic matter increased from values around Redfield (6.6) to ~8–13, which is beneficial for potential carbon dioxide removal. On the other hand, sinking matter was remineralized at faster rates and showed lower sinking velocities, which led to shallower remineralization depths. Particle properties were more favorable for deep carbon export in the recurring upwelling mode, while in the singular mode the C:N increase of sinking matter was more pronounced. In both upwelling modes roughly half of the produced organic carbon was retained in the water column until the end of the experiment. This suggests that the plankton communities were still in the process of adjustment, possibly due to the different response times of producers and consumers. There is thus a need for studies with longer experimental durations to quantify the responses of fully adjusted communities. Finally, our results revealed that artificial upwelling affects a variety of sinking particle properties, and that the intensity and mode with which it is applied control the strength of the effects.

Keywords: artificial upwelling, export flux, particle properties, sinking velocity, remineralization rate, remineralization depth, carbon sequestration, mesocosm study

INTRODUCTION

To limit global warming to between 1.5 and 2°C as committed in the Paris Climate Agreement, reducing carbon dioxide (CO₂) emissions alone will most likely not suffice. Negative emission technologies, which actively remove CO₂ from the atmosphere, will be needed to achieve net zero CO₂ emissions (IPCC, 2018). Many such technologies focus on the ocean (GESAMP, 2019), which has the capacity to potentially store large amounts of extra carbon (Sabine et al., 2004). The world ocean has already absorbed roughly a third of cumulated anthropogenic CO₂ emissions (Khatiwala et al., 2013), thereby mitigating a substantial part of global warming. The ocean's storage capacity might be further enhanced by strengthening the carbon flux from the air-sea-interface to the deep ocean. One component of this flux is the biological carbon pump, which mediates the transport of organic carbon produced in the euphotic zone to the deep ocean. Once the carbon reaches the deep ocean, it remains out of touch with the atmosphere for decades to centuries (i.e., sequestered, Boyd et al., 2019). Some negative emission technologies focus on strengthening the biological carbon pump to enhance this natural carbon sink. In the oligotrophic ocean, increased vertical mixing and resulting nutrient-upwelling can enhance carbon fluxes to the deep ocean (Pedrosa-Pàmies et al., 2019). This principle is utilized by a negative emission technology called “artificial upwelling,” an approach in which nutrient- and CO₂-rich deep ocean water is pumped to the surface layer with the goal of enhancing primary production and hence, carbon export.

The feasibility of artificial upwelling as a CO₂-sequestration technique has been disputed by several modeling studies. Although it has the potential to sequester additional atmospheric carbon (Yool et al., 2009), Pan et al. (2015) found this potential to be rather small and connected to very high efforts; i.e., the upwelling of massive amounts of water (117 Sv) from 1,000 m depth would achieve an additional oceanic CO₂ uptake of 1 Gt C yr⁻¹. For comparison, in the year 2008 the oceans took up ~2.5 Gt of anthropogenic carbon (Khatiwala et al., 2009). Furthermore, modeling studies have suggested that geophysical ocean-atmosphere feedbacks might lead to undesirable side-effects, e.g., that stopping artificial upwelling after several decades of large-scale operation would increase global temperatures to levels higher than if it had not been applied at all (Oschlies et al., 2010; Keller et al., 2014; Kwiatkowski et al., 2015). Beside such geophysical feedbacks, other major unknowns are the biological and biogeochemical responses of pelagic communities to artificial upwelling. Basically all our knowledge about potential effects of artificial upwelling is based on models with a low degree of ecological complexity and simplified biogeochemistry (e.g., constant stoichiometry and particle properties). So far, there is little empirical research on the effects of artificial upwelling on the ecology and biogeochemistry of pelagic plankton communities.

The limited number of experimental studies so far have shown that artificial upwelling can significantly increase phytoplankton biomass in oligotrophic waters (McAndrew et al., 2007; Strohmeier et al., 2015; Giraud et al., 2016, 2019; Casareto et al., 2017). However, studies considering its effect on the export

production and carbon sequestration processes are scarce, mostly due to the methodological difficulties of simulating artificial upwelling under close-to-natural conditions. Svensen et al. (2002) carried out a mesocosm nutrient enrichment experiment, in which they found that nutrient enrichment increases particulate organic carbon (POC) sedimentation and that the effect size is dependent on the frequency of nutrient additions. However, no study so far has examined in detail the properties of sinking particles, particularly sinking velocity and degradation rates, which together determine the remineralization depth and thus the potential for deep carbon export.

To create a net carbon sink using artificial upwelling, the export flux needs to overcompensate for the CO₂ upwelled with deep water (Pan et al., 2016). The most important export conditions determining carbon sequestration potential are (i) elemental stoichiometry of sinking particles and (ii) the remineralization depth of these particles. While artificially upwelled deep water usually contains more nitrogen and phosphorus than the surface water, it also contains more dissolved inorganic carbon (DIC), which could potentially outgas to the atmosphere. Hence, for artificial upwelling to increase the ocean's function as a net carbon sink, more carbon must be sequestered than is brought up as excess DIC (excess DIC = deep water DIC – surface water DIC). Carbon sequestration is thereby promoted by a high C:N ratio of sequestered particulate material (POC:PON). How much of the exported matter reaches the sequestration depth (i.e., the depth at which sinking material is regarded as sequestered) is determined by the remineralization length scale (RLS). It is a proxy for how deep particles can sink before being remineralized. Both parameters are dependent on the plankton community that develops as a response to artificial upwelling. Plankton community composition shapes not only the magnitude and C:N stoichiometry of the mass flux (Taucher et al., 2021), but also the characteristics of the sinking particles, such as their sinking velocities (SV) and carbon-specific remineralization rates (C_{remin}) (e.g., Legendre and Rivkin, 2002; Iversen and Ploug, 2010; Henson et al., 2012b; Turner, 2015; Bach et al., 2019). Community composition and succession are in turn controlled by the amount of added nutrients and the frequency with which they are supplied (Leibold et al., 1997; Jakobsen et al., 2015). This is why the intensity of artificial upwelling, as well as the mode of the application (i.e., the frequency of deep water addition) are important parameters that impact the export of organic matter.

Here, we present results from a mesocosm experiment where we studied the impact of different intensities and modes of artificial upwelling on arising food web dynamics and particulate matter export. We addressed the question whether increasing intensity of artificial upwelling leads to a higher mass flux and increased potential for carbon sequestration. Additionally, we compared the particle properties and their implications for deep carbon export of a singular upwelling event with a recurring mode of upwelling. The singular upwelling mode resembled an application of artificial upwelling that fertilizes each patch of water only once, e.g., by means of a moored wave pump (see e.g., Liu et al., 1999; Fan et al., 2016). The recurring mode on the

other hand resembled an approach where the upwelling device drifts within a patch of water and fertilizes it over longer periods of time. Mesocosms are useful to study effects on whole pelagic communities, since they incorporate the responses of multiple trophic levels of a food web and allow for the assessment of a variety of ecological and biogeochemical parameters in an enclosed and well-characterized (eco-) system. Our study is the first to analyze the combined effects of upwelling intensity and upwelling mode on pelagic communities.

MATERIALS AND METHODS

Experimental Setup

The mesocosm experiment was conducted from 5th of November 2018 and lasted for 39 days. Nine Kiel Off-Shore Mesocosms for Ocean Simulations (KOSMOS, see Riebesell et al., 2013 for technical information) were deployed in Gando Bay off the east coast of Gran Canaria (27°55.673' N, 15°21.870' W). They enabled us to monitor the temporal development of the enclosed pelagic communities at *in situ* conditions. The mesocosms contained a 15 m long water column with a volume of ~38 m³. We simulated artificial upwelling by replacing part of the oligotrophic mesocosm water with nutrient rich deep water. Our experimental design comprised one mesocosm as a control (i.e., no deep water addition), while the remaining eight received deep water additions in different modes and intensities. Four of these mesocosms were fertilized once with one big addition at the beginning of our study, i.e., the “singular treatments.” The other four were fertilized eight times throughout the experiment with lower amounts of deep water per addition, but comparable total amounts of deep water summed up over the study period, i.e., the “recurring treatments.” Both addition modes had four different levels of mixing ratio (low, medium, high, and extreme), with two respective mesocosms of different modes receiving similar amounts of deep water in total (Table 1).

We collected deep water for fertilization off the coast of Gran Canaria using a deep water collector, an opaque synthetic bag with 100 m³ carrying capacity (see Taucher et al., 2017 for technical details), and moored it at the mesocosm site after each of two collections. The water was supposed to originate from ~600 m depth, where NO₃⁻ concentrations are as high as 20–25 μmol L⁻¹ (Llinás et al., 1994), in order to enhance primary and export production. However, due to loss of equipment under rough conditions we could not as planned collect water from that depth. Instead, we collected water from 330 m depth on the 26th of October 2018 (experimental day -10 = T-10) and from 280 m depth on the 28th of November (T23). Therefore, to reach the macronutrient concentrations necessary to achieve our planned experimental fertilization, we added nitrate (NO₃⁻), phosphate (PO₄³⁻) and silicate [Si(OH)₄] to the deep water prior to the first addition, resulting in concentrations of 25, 1.38, and 12.1 μmol L⁻¹, respectively. We calculated the amount of new N added to the mesocosms in the course of the whole experiment (Table 1) by calculating and adding up the net N inputs of each deep water replacement. For more details on the experimental setup and mesocosm activities (see Sswat et al., in prep.).

Sampling Procedure and Maintenance

Sampling for various parameters was generally carried out every second day (see Figure 1). A higher sampling frequency was pursued at the beginning of the experiment in order to cover the biological responses to the first two deep water additions in higher temporal resolution. The samples were either analyzed at our on-shore lab facilities at the Oceanic Platform of the Canary Islands (PLOCAN), the Marine Science and Technology Park (Parque Científico Tecnológico Marino, PCTM) or the University of Las Palmas (ULPGC), or transported back to Kiel for analysis at the GEOMAR Helmholtz Centre for Ocean Research Kiel.

A CTD60M (Sea & Sun Technology GmbH, Trappenkamp, Germany) was cast to get depth profiles for temperature, salinity, density, pH, turbidity, oxygen (O₂) and photosynthetically active radiation. Bulk samples from the upper 13 m of the water column (WC) were taken for the analysis of primary productivity, chlorophyll *a* (Chl *a*), photosynthetic pigments, phyto- and microzooplankton analysis, prokaryotic heterotrophic production (PHP), and for the analysis of suspended particulate matter (PM_{WC}). The latter was composed of particulate organic and inorganic carbon (POC_{WC}/PIC_{WC}), particulate organic nitrogen (PON_{WC}) and phosphorus (POP_{WC}), and biogenic silica (BSi_{WC}). Bulk samples were collected with integrated water samplers (HYDRO-BIOS Apparatebau GmbH, Kiel, Germany), which performed depth-integrated sampling from the upper 13 m of the water column. On each sampling day, around 40–60 L of bulk samples (i.e., 8–12 water samplers) were sampled per mesocosm. These were filled into 10 L carboys and stored dark and cool until arrival in the on-shore labs. Dissolved nutrients and carbonate chemistry (DIC and total alkalinity) were also sampled from the integrated water samplers.

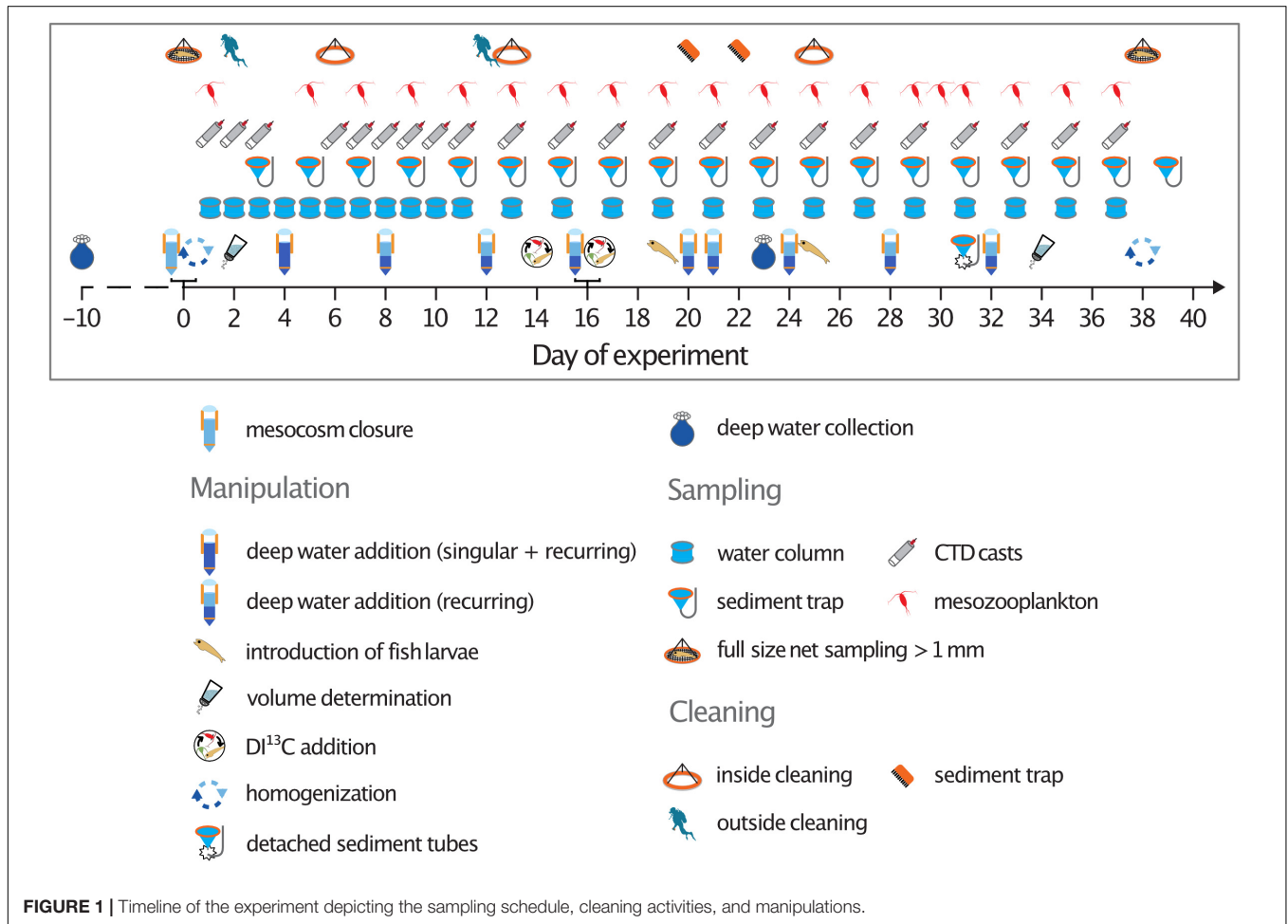
Sedimented particulate matter was pumped out of the sediment trap (depth = 15 m) with a manual vacuum pump, not exceeding 0.3 bar during the process. Sediments were collected in 5 L glass bottles (Schott Scandinavia A/S, Kgs. Lyngby, Denmark) and stored in darkness until arrival in the lab, where they were subsampled for various parameters. The bottles were gently rotated to resuspend the material before homogeneous subsamples were taken. These subsamples were used for particle sinking velocity measurements and measurements of carbon-specific remineralization rates. For the latter, seven glass bottles (Schott, 310 mL volume) were additionally sampled with mesocosm water without headspace. They were used for incubating the sediment subsamples. The remaining sediment sample was weighed and analyzed for particulate carbon, nitrogen, phosphorus and biogenic silica content (see Boxhammer et al., 2016 for details of the method).

To prevent wall growth on the inside walls of the mesocosms, a ring-shaped wiper was pulled through each mesocosm roughly every 10 days (see Figure 1). This counteracted nutrient consumption by fouling organisms and their alteration of incoming light. For the latter reason, also the outside walls were cleaned twice during the study by divers equipped with brushes.

The sediment tubes of all mesocosms detached from the sediment traps on T30 due to strong winds and currents. They were reinforced and refitted on T31, however, no sediment

TABLE 1 | Treatment overview indicating different upwelling modes and intensities, mean net volume exchange of surface water with nutrient-rich deep water per addition and the total amount of new nitrogen that was added via the addition of deep water throughout the experiment.

Upwelling mode	Control		Singular				Recurring			
	–	Low	Medium	High	Extreme	Low	Medium	High	Extreme	
Volume exchange per addition (%)	0	6.4	12.0	22.4	39.2	0.8	1.6	3.2	6.4	
Total new N added ($\mu\text{mol L}^{-1}$)	0	1.6	3.1	5.6	9.8	1.6	3.1	6.2	11.0	



samples could be recovered that day and thus sedimented matter elemental composition, sinking velocity and remineralization rate could not be measured on T31. The tubes of the singular medium and high treatments and of the recurring extreme treatment disconnected again and had to be reattached a second time on T33. We were not able to sample the singular medium treatment that day, and the singular high and recurring extreme treatments had short incubation periods of only 18 h between the T33 and T35 samplings. We discarded all sinking velocity measurements from these days, since they showed systematically higher values than the measurements of the surrounding days. The mean seawater density inside all mesocosms between 0.5 and 15 m was slightly higher than in the surrounding water (1025.69 ± 0.11 and $1025.42 \text{ kg m}^{-3}$ on T31, respectively), so

that we assume no Atlantic water entered the small opening at the base of the sediment trap ($\varnothing \sim 1 \text{ cm}$). An outflow of mesocosm water into the surrounding seems more likely under these circumstances. Nevertheless, we cannot rule out the possibility that e.g., due to wave and current action some Atlantic water entered the mesocosms. The surrounding water was, however, oligotrophic, and had substantially lower POC concentrations than any of the mesocosms on T33 according to our measurements ($7.9 \mu\text{mol POC L}^{-1}$ in the Atlantic water compared to $35.7 \pm 21.4 \mu\text{mol POC L}^{-1}$ in the mesocosms). This makes an influential contamination with biogenic material and/or species from the outside less probable, even if Atlantic water had entered the mesocosms. At the end of the experiment the water column in the mesocosms was mixed by pumping

compressed air through the sediment hose. This might have altered the sediment flux and quality of the last sampling on T39.

Sample Processing and Measurement

Sediment Trap Material

At PLOCAN the sediment trap (ST) material was prepared for elemental analysis of POC_{ST} , PON_{ST} , and BSi_{ST} by first of all separating the particles from the seawater. 3 mol L^{-1} ferric chloride (FeCl_3) were added to each 5 L bottle of sediment material to enhance flocculation and coagulation, followed by 3 mol L^{-1} NaOH addition to compensate for the decrease in pH (as described in detail in Boxhammer et al., 2016). After letting the material settle for 1 h, the supernatant was gently decanted. The remaining flocculated material was then centrifuged for 10 min at $\sim 5,200 \text{ g}$ in a 6–16KS centrifuge (Sigma Laborzentrifugen GmbH, Osterode am Harz, Germany). An additional 10 min centrifugation step at $\sim 5,000 \text{ g}$ in a 3K12 centrifuge (Sigma) resulted in compact sediment pellets, which were frozen at -20°C and transported to Kiel for further processing. In Kiel, the pellets were freeze-dried to remove any leftover moisture and then ground in a cell mill (Edmund Bühler GmbH, Bodelshausen, Germany) to a fine homogeneous powder that was suitable for subsampling and further elemental analysis (Boxhammer et al., 2016). Subsamples for POC/N were weighed into tin capsules, acidified with 1 mol L^{-1} HCl, dried over night at 50°C , and then measured in duplicate on a CN analyzer (Euro EA-CN, HEKAtech GmbH, Wegberg, Germany) according to Sharp (1974). To determine BSi concentrations, $\sim 2 \text{ mg}$ subsamples of the sediment powder were measured spectrophotometrically following Hansen and Koroleff (1999).

The sediment powder was stored dark and cool in glass vials. As some samples required multiple vials due to their high amounts, subsamples from all bottles were measured for each variable. If they differed among each other in elemental composition, the sample was pooled, homogenized, split up and remeasured until all bottles yielded the same results.

Water Column Samples

Water column samples were subsampled for elemental ($\text{POC}_{\text{WC}}/\text{PON}_{\text{WC}}$) and pigment analysis (Chlorophyll *a*/Chl *a*) by collection on pre-combusted glass fiber filters ($0.7 \mu\text{m}$, Whatman) in our on-shore labs. POC and PON filters were acidified for $\sim 2 \text{ h}$ to remove inorganic carbon, using 1 mol L^{-1} HCl, and dried over night at 60°C in pre-combusted glass petri dishes. Filters for total particulate carbon (TPC) were dried without prior acidification. All filters were packed in tin cups ($8 \times 8 \times 15 \text{ mm}$, LabNeed GmbH, Nidderau, Germany) and measured back in Kiel on a CN analyzer (Euro EA-CN, HEKAtech) as described for sediment C and N content above. Due to sample handling and/or measurement errors, measured POC_{WC} concentrations were sometimes higher than those of TPC_{WC} . Whenever the difference was greater than 10%, we report the TPC_{WC} instead of the POC_{WC} concentration (i.e., assuming that no PIC was present). Samples for Chl *a* were stored at -80°C in cryovials until analysis in Kiel. They were extracted in acetone (100%) and homogenized with glass beads in a cell mill. After centrifugation (10 min, $5,200 \text{ rpm}$, 4°C) they were

filtered through $0.2 \mu\text{m}$ PTFE filters (VWR International GmbH, Darmstadt, Germany). Phytoplankton pigments, including Chl *a* in the supernatant were measured by an HPLC Ultimate 3,000 (Thermo Scientific GmbH, Schwerte, Germany).

Primary productivity was measured in the on-shore labs using a modified Nielsen (1952) ^{14}C uptake method described by Cermeño et al. (2012). Four water column subsamples (70 mL) per mesocosm were prefiltered and peaked with $2.96 \cdot 10^5 \text{ Bq}$ of ^{14}C -labeled sodium bicarbonate solution ($\text{NaH}^{14}\text{CO}_3$, PerkinElmer Inc., Waltham, United States). They were subsequently incubated *in vitro* for 24 h in a 12 h dark-light cycle. One of the subsamples was thereby covered with an opaque foil in order to measure the dark carbon uptake. Light intensity and temperature were set to *in situ* conditions based on CTD measurements. Thereafter, size fractions were filtered, the PIC and DIC fractions removed through acidification and the filters and filtrates were treated with a scintillation cocktail (Ultima Gold XR). Disintegrations per minute were counted on a scintillation counter (Beckmann LS-6500, Beckman Coulter Inc., Brea, United States). From these, knowing the concentration of added ^{14}C isotope and the measured *in situ* DIC concentration (see paragraph on DIC below), primary productivity rates ($\mu\text{mol C L}^{-1} \text{ d}^{-1}$) were calculated. For a more detailed description of the sampling and measurement procedure see Ortiz et al. (submitted).

PHP was estimated from rates of protein synthesis determined by the incorporation of tritiated leucine [^3H]leucine; Perkin Elmer] using the centrifugation method (Smith and Azam, 1992). Four subsamples (1 mL) and two trichloroacetic acid killed blanks were dispensed into screw-cap Eppendorf tubes. They were spiked with [^3H]leucine (final concentration: 20 nmol L^{-1} , specific activity 123 Ci mmol^{-1}) and incubated at *in situ* temperature (21°C) in the dark for 2–3 h. After the incubation, $100 \mu\text{L}$ of 50% trichloroacetic acid were added to the subsamples, which were kept with the blanks at -20°C until centrifugation at $12,000 \text{ rpm}$ for 20 min. The supernatant was carefully removed, and 1 mL of scintillation cocktail (Ultima Gold XR) was added to the Eppendorf tubes. They were stored in darkness for 24 h, after which the incorporated radioactivity was determined on a scintillation counter (Beckmann LS-6500). PHP was calculated using a conservative theoretical conversion factor of $1.55 \text{ kg C mol}^{-1} \text{ Leu}$ assuming no internal isotope dilution (Kirchman and Ducklow, 1993).

Samples for dissolved inorganic nutrients were filtered ($0.45 \mu\text{m}$ Sterivex filters, Merck KGaA, Darmstadt, Germany) upon arrival in the on-shore lab. Nitrate (NO_3^-), nitrite (NO_2^-), ammonium (NH_4^+), phosphate (PO_4^{3-}) and silicic acid [$\text{Si}(\text{OH})_4$] concentrations were subsequently measured spectrophotometrically on a five channel continuous flow analyzer (QuAAtro AutoAnalyzer, SEAL Analytical Inc., Mequon, United States).

Samples for DIC measurements were filtered to remove particulate inorganic carbon ($0.7 \mu\text{m}$, Whatman) with an overflow of 1.5 times the volume of the filtrate. Inclusion of air in the filtration process was carefully avoided. The filtrate was fixed with mercuric chloride (HgCl_2). DIC

concentrations were measured in triplicate on an AIRICA system (MARIANDA, Kiel, Germany) in Kiel, using a LI-COR LI-7000 Analyzer (LI-COR Biosciences GmbH, Bad Homburg, Germany). Certified reference materials (CRM batch 142, supplied by A. Dickson, Scripps Institution of Oceanography, United States) were used to determine the accuracy of DIC measurements.

Dissolved organic carbon (DOC) samples were filtered through pre-combusted GF/F filters (450°C, 6 h) into polypropylene copolymer Nalgene™ bottles (Thermo Scientific), and stored at −20°C. Prior to analysis, samples were acidified to a pH < 2 to remove inorganic carbon. Subsequently, DOC concentrations were measured by high temperature catalytic oxidation on a total organic carbon analyzer (TOC-V, Shimadzu Europa GmbH, Duisburg, Germany). The instrument was calibrated daily using potassium hydrogen phthalate (99.95–100.05%, p.a., Merck), which yielded an analytical precision of $\pm 1 \mu\text{mol C L}^{-1}$. The accuracy was determined using certified reference materials (provided by D. A. Hansell, University of Miami, United States). Measured CRM concentrations were $43.39 \pm 0.92 \mu\text{mol C L}^{-1}$ ($n = 33$), at a reference value of $42\text{--}45 \mu\text{mol C L}^{-1}$.

Sinking Velocity of Sediment Trap Particles

Sinking velocity and remineralization rates of sedimented particulate matter were measured in a temperature-controlled on-shore lab at PCTM. Sinking velocity was determined by video microscopy using the method described in Bach et al. (2012). Sediment subsamples were diluted with filtered seawater according to their particle density (1:25–1:100) and injected to a sinking chamber (a cuvette with the dimensions: $10 \times 10 \times 350 \text{ mm}$), which was mounted vertically on a FlowCam 8000 (Fluid Imaging Technologies Inc., Scarborough, United States). Gravitational settling of particles in the cuvette was subsequently monitored for 20 min. Measurements were carried out at *in situ* temperatures ($\sim 21^\circ\text{C}$) under ventilation to prevent a temperature gradient around the sinking chamber. Particles between 25 and $1,000 \mu\text{m}$ were identified at a frame rate of 15–20 fps. The FlowCam measures more than 60 visually assessed parameters, which were read into MATLAB (version R2018b) for data analysis. The MATLAB script described by Bach et al. (2012 see: “Evaluation of sinking velocities”) was adjusted for the more recent FlowCam version and used for calculation of sinking velocities. By finding multiple captures of the same particle on a y-position-gradient and applying a linear regression model against time, sinking velocities were calculated. They were corrected for wall effects of the sinking chamber according to the equation given by Ristow (1997). Further data analysis was carried out with the programming software R (R Core Team, 2017) using RStudio (version 1.3.959) and the package “tidyverse” (Wickham et al., 2019). An optical proxy for particle porosity (P_{int}) was calculated according to Bach et al. (2019). It is essentially a measure of the brightness of a particle, scaled with its size.

Analysis of the distribution of sinking particle volume showed that most of the volume was contained in a small fraction of particles with high equivalent spherical diameter (ESD) in all measurements (largest 10% accounted for > 75% of total particle biovolume). The smaller size fractions, however, constituted the majority of particle counts ($\sim 90\%$ in the 25–200 μm fraction). To not give the more numerous small particles undue weight, we calculated a “weighted SV.” It gives more weight to the high-volume, but underrepresented bigger particles, which consequently contain more biomass (see **Supplementary Figure 2** for an illustration of weighted SV calculation). In order to do so, we determined the ESD for which at least 25% of the summed-up particle volume was contained in the smaller particles and 75% in the bigger ones. For this “weighted ESD” we calculated the corresponding “weighted SV” by fitting a linear model to the mean sinking velocities as a function of their ESD across different size classes (log-spaced). We used size class means to—again—not give the numerous small particles undue weight. This weighted sinking velocity (hereinafter referred to as sinking velocity or SV) is thus the sinking velocity that corresponds to the ESD which segments the measurement into two particle volume fractions containing 25 and 75% of the total particle volume. We calculated the “weighted particle porosity” in the same way (hereinafter referred to as porosity or P_{int}). We used the weighted SV for all following sinking velocity dependent calculations such as the remineralization length scale (see below).

Remineralization Rates of Sinking Particles

Remineralization rates were determined every 4–6 days. We therefore took water column samples, collected in four replicate and three control bottles per mesocosm [(4 + 3) bottles \times 9 mesocosms = 63 bottles in total]. They were transported back to the temperature-controlled lab (set to *in situ* temperature based on CTD measurements), where they acclimatized in a water bath for 2 h. Then, 0.5–3 mL of sediment subsample of the respective mesocosm were added to the four replicate bottles. The control bottles were left untreated. To examine the rate at which sedimented POC was remineralized back to DIC, all bottles were incubated in the dark on a rotating plankton wheel ($\sim 1 \text{ rpm}$) and Oxygen depletion over time was measured. O_2 measurements were carried out using a handheld optical measurement device (Fibox4 Trace, PreSens—Precision Sensing GmbH, Regensburg, Germany), measuring non-invasively on PSt3 optodes (PreSens) mounted inside the bottles. O_2 measurements were automatically corrected for temperature (measured in a dummy bottle) and atmospheric pressure by the Fibox4. We adjusted the optode salinity correction according to the daily observed salinity measurements of the CTD cast. The second O_2 measurement was carried out after the bottles had been mixed properly, about 2 h after the incubation start, and were repeated continuously in 2–6 h intervals. The incubations lasted between 19 and 43 h, during which O_2 measurements were done at least 7 and up to 16 times. Particles in the incubation bottles were then collected on pre-combusted glass fiber filters (0.7 μm , Whatman) and

analyzed for their POC content the same way as the water column POC filters.

By dividing the O_2 consumption rate (r in $\mu\text{mol } O_2 \text{ L}^{-1} \text{ d}^{-1}$) of the sedimented matter by its POC content at the end of the incubation ($\mu\text{mol C L}^{-1}$), the carbon-specific remineralization rate of the sedimented particulate matter (C_{remin} in d^{-1}) was calculated according to:

$$C_{\text{remin}} = \frac{(r * RQ)}{(POC + r * RQ * \Delta t)}$$

where RQ is the respiratory quotient ($\mu\text{mol C } \mu\text{mol } O_2^{-1}$), which is commonly used as 1-mol CO_2 produced:1-mol O_2 consumed (= 1) (Ploug and Grossart, 2000; Iversen and Ploug, 2013; Bach et al., 2019) and Δt (d) as the time interval from the start of the incubation until the start of the filtration. In order to distinguish the response of the sedimented matter from any background seawater oxygen consumption, the C_{remin} rates of the sediment-containing bottles were corrected for the mean C_{remin} rates in the blank bottles.

Calculation of Export Flux and Remineralization Depth

The mass flux to the sediment trap (POC_{ST} , PON_{ST} , BSi_{ST}) was calculated for each element from the amount measured in the sediment powder. The total content per sample was calculated and normalized to the volume of the mesocosm and the time between sample collection (48 h), which yielded the daily mass flux in μmol per liter mesocosm water ($\mu\text{mol L}^{-1} \text{ d}^{-1}$). Ten data points were missing due to the detachment of the sediment trap hoses on and around T30 (all mesocosms on T31 and the singular medium mesocosm on T33, see section “Sampling Procedure and Maintenance”). To calculate the cumulative POC_{ST} flux (ΣPOC_{ST}), daily POC_{ST} fluxes were summed up, whereby the missing data points were interpolated using the two surrounding data points (T29 and T33, or T29 and T35 for the singular medium treatment). Cumulative mass fluxes are reported in $\mu\text{mol L}^{-1}$.

To find out how much of the produced organic carbon had been exported from the water column until a specific experimental day (Tx), total organic carbon in the water column (TOC_{WC}) was calculated, subtracted by the initial TOC_{WC} concentration on T01 (= ΔTOC_{WC}), and finally compared to the cumulative POC_{ST} flux (ΣPOC_{ST}).

$$\frac{\Delta TOC_{\text{WC}}(Tx)}{POC_{\text{ST}}(Tx)} = \frac{(POC_{\text{WC}}(Tx) + DOC_{\text{WC}}(Tx)) - (POC_{\text{WC}}(T01) + DOC_{\text{WC}}(T01))}{POC_{\text{ST}}(Tx)}$$

Finally, the remineralization length scale (RLS, i.e., remineralization depth) was calculated, which is the quotient of sinking velocity and carbon specific remineralization rate.

$$RLS = \frac{SV}{C_{\text{remin}}}$$

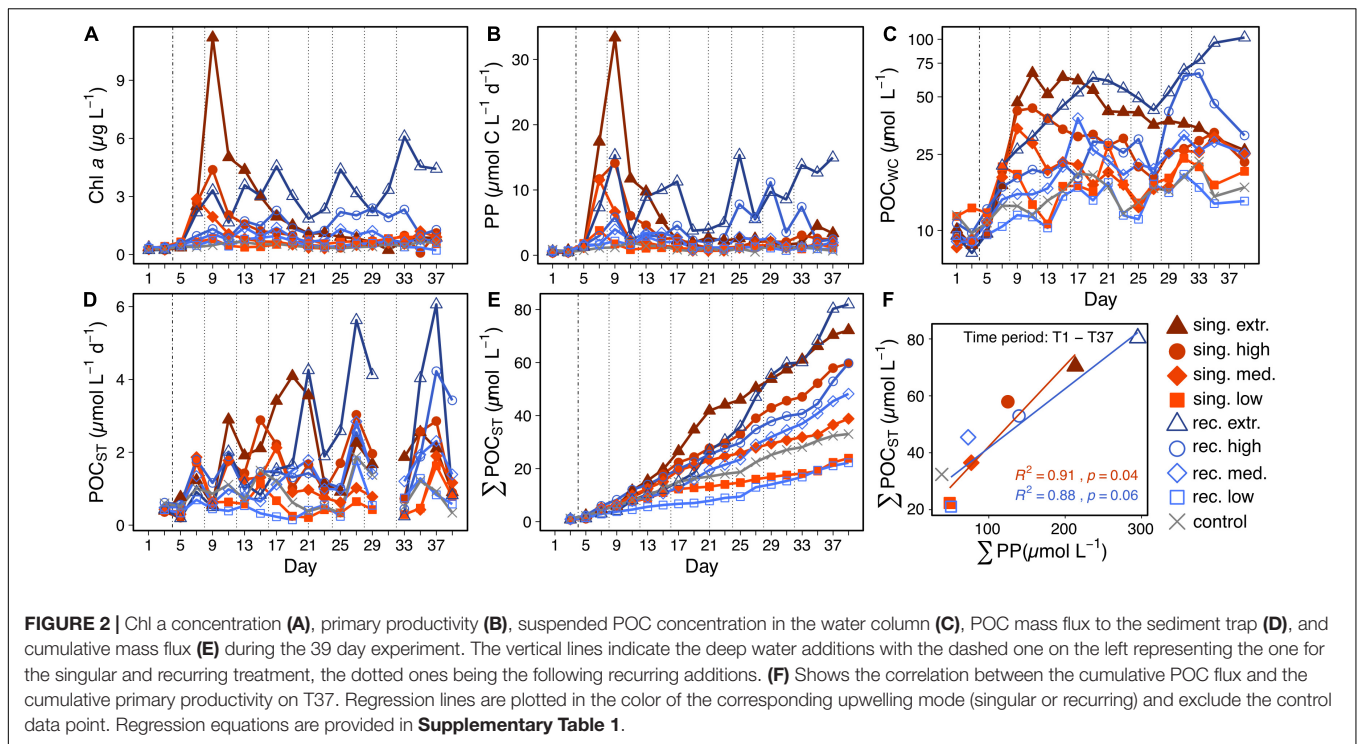
It is the depth (m) by which 63% of the sinking organic particle flux have been remineralized (Cavan et al., 2017) and thus a proxy for the POC transfer efficiency to depth.

RESULTS

Primary Production, Export Flux, and Stoichiometry

Primary productivity as well as Chl *a* and POC_{WC} concentrations increased in all treatment mesocosms following the first deep water addition on T4. Phytoplankton blooms dominated by diatoms (Ortiz et al., submitted) developed in the singular treatments with intensity and duration depending on their upwelling intensity. The highest phytoplankton biomass (measured as Chl *a* concentration) was observed in the extreme singular treatment ($11.2 \mu\text{g L}^{-1}$ on T9). Recurring upwelling sustained more stable phytoplankton biomass and productivity compared to singular upwelling. In the high and extreme recurring treatments primary productivity rates increased until well into the second half of the experiment (Figures 2A,B). Note that in most mesocosms a large fraction of produced organic matter was retained in the water column as suspended POC_{WC} at the end of the experiment (Figure 2C). This was particularly evident in the recurring treatments, which received nutrients until T32. In the extreme recurring treatment, the amount of POC_{WC} at the end of the experiment was higher than its total cumulative POC mass flux (Figures 2C,E: $102 \mu\text{mol L}^{-1} POC_{\text{WC}}$ vs. $82 \mu\text{mol L}^{-1}$ of cumulative POC_{ST} , on T39).

The treatment differences observed in Chl *a* and primary productivity were mirrored in the POC mass flux. A post-bloom export event occurred in the singular treatments 4–10 days after their bloom peak in the water column, with the time lag being longer at higher intensities of deep water addition. This is based on visual inspection (comparison of Figures 2B,D, e.g., extreme singular treatment bloom peak on T9, highest POC_{ST} flux between T17–T21), since the temporal variation in the POC_{ST} data did not allow a reliable calculation of time lags as e.g., in Stange et al. (2017). In contrast, the recurring mode led to POC_{ST} maxima 20–30 days after initial fertilization (Figure 2D). In both modes, the overall cumulated POC_{ST} at the end of the experiment correlated positively with the cumulated primary productivity (Figure 2F). The control mesocosm was excluded from this regression analysis, because it had unexplainably high export rates, although it did not receive any new N via deep water addition. When comparing the total amount of dissolved and particulate N at the beginning and end of the study period in the control, we found that approx. $4.2 \mu\text{mol L}^{-1}$ N sank out to the sediment trap, which were not accounted for in the initial N pools, according to our measurements. Apparently, there was an N source (or multiple) in the control, which we did not capture, e.g., fouling residues on the inside walls of the sediment trap or large swimmers (zooplankton, small fish), which were initially present but not accounted for. Other causes for the discrepancy might have been methodology-related, e.g., inaccurate sampling of patchily distributed PON_{WC} . Regarding the test statistics, removing the control from the quantitative regression analysis in Figure 2F decreased the *p*-values (from 0.014 to 0.044 in the singular and from 0.015 to 0.060 in the recurring upwelling mode) and did not considerably affect the *R*-values (from 0.90 to



0.91 in the singular and from 0.89 to 0.88 in the recurring (upwelling mode).

The peaks in POC_{ST} on T7 and T27 (Figure 2D) in all mesocosms likely occurred due to the preceding cleaning of the inside mesocosm walls on T6 and T25, respectively. It appears that a carbon-rich biofilm was growing on the walls, which was removed during cleaning and subsequently sank into the sediment traps. This is also indicated by the high C:N ratios of POC flux on these days (compare Figures 2D, 3A). On T33 and T39, POC_{ST} was lower than expected for most mesocosms, contrasting the time points before and after these days. For T33, the reason for this was probably a lower than usual accumulation period of material due to the preceding sediment tube detachments (see section “Sampling Procedure and Maintenance”). Many large and heavy particles might have sunk out before the reattachment of the tubes, leaving a higher proportion of slower sinking particles with lower POC content for the accumulation period. Regarding T39, the final fish net haul and the mixing of the water column through the sediment hose on T38 likely caused lower sedimentation rates of organic matter. The fish net haul by removing large and sticky aggregates, the mixing by resuspending already settled material.

In all treatment mesocosms except for the recurring low treatment more organic carbon was retained in the water column as POC and DOC than exported to the sediment trap as POC (ratio between $\Sigma\text{POC}_{\text{ST}}$ and $\Delta\text{TOC}_{\text{WC}} < 1$). The ratios did not substantially differ among the singular treatments, whereas they decreased with increasing upwelling intensity in the recurring mode (Table 2).

In the singular upwelling treatments, the C:N ratios in the suspended particulate matter pool generally increased to

higher than Redfield ratios on T11, 1 week after the deep water addition (Figure 3B). This occurred precisely when the blooming phytoplankton communities became nutrient limited (see Supplementary Figure 1 for inorganic nutrient concentrations), and was particularly prominent under high upwelling intensities. In the recurring treatments, the C:N ratios of POM_{WC} showed a high temporal variation, they, however, tended to increase throughout the study period.

The C:N ratio of the mass flux was higher than the canonical Redfield ratio of 6.6 in all mesocosms throughout the experiment (Figure 3A). Increasing amounts of deep water addition, however, enhanced the mass flux C:N further. We found a positive correlation between N addition and the C:N of the mass flux in the singular treatment between T11 and T21, when most of the post-bloom flux occurred (Figure 3C). Furthermore, the Si:C ratio during this time was higher in the singular treatments compared to the recurring ones and the control (Figure 3D).

Particle Properties and Remineralization Depth

Remineralization rates of sinking particles ranged from 0.09 to 0.12 d^{-1} initially, and peaked in most mesocosms a week after the first deep water addition (T11). Thereafter, they decreased in all treatments (Figure 4A). Sinking velocities were generally lower in the singular treatments than in the recurring ones (Figure 4B). This difference between the two modes was confirmed by a *t*-test for mean sinking velocities calculated for days T7–T15 [two-sample $t(6) = -4.019$, $p = 0.007$]. Low sinking velocities in the singular mode were accompanied by high porosities in

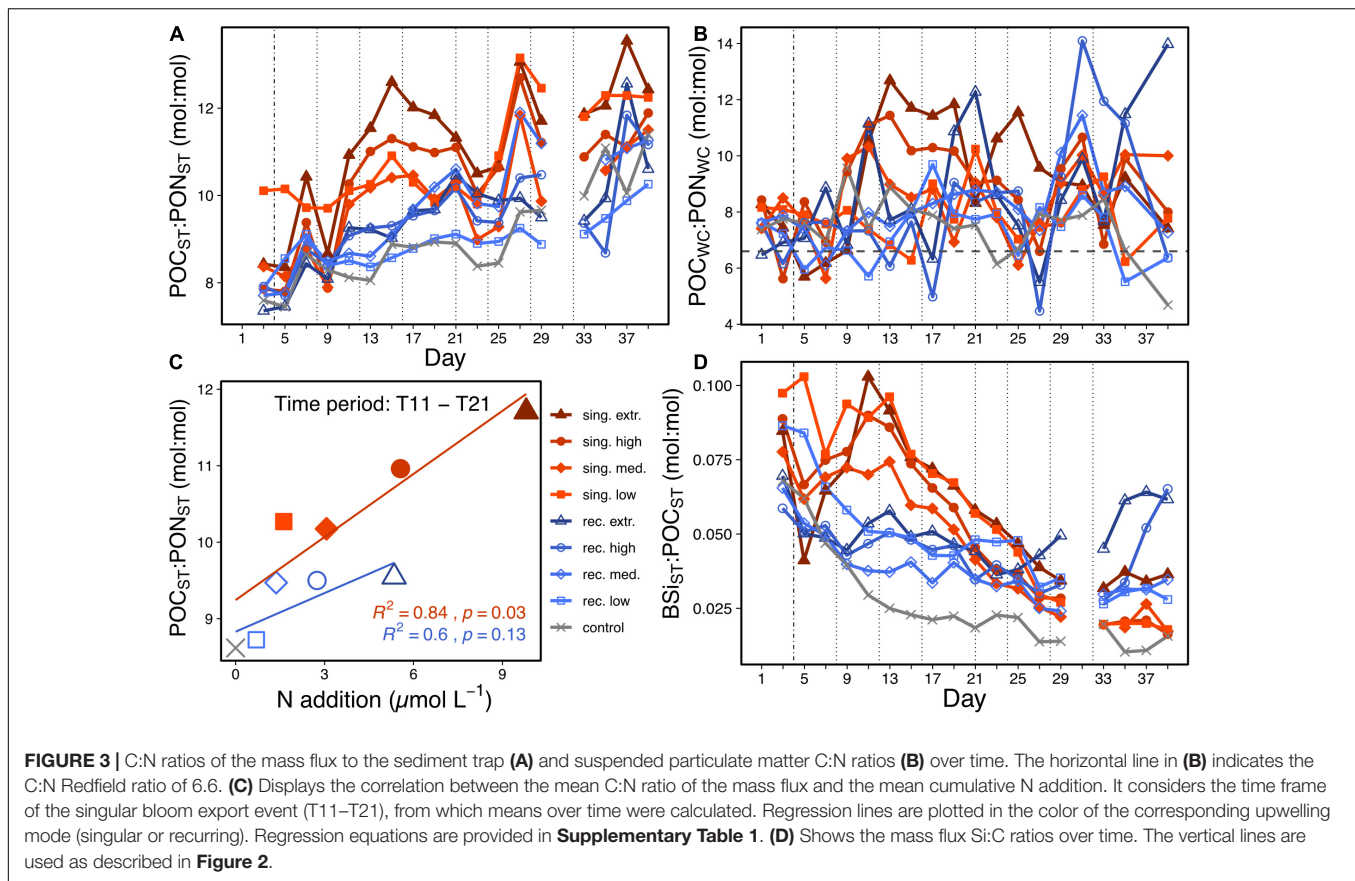


TABLE 2 | Mean $\Delta\text{TOC}_{\text{WC}}$ and $\Sigma\text{POC}_{\text{ST}}$ values, as well as $\Delta\text{TOC}_{\text{WC}}:\Sigma\text{POC}_{\text{ST}}$ ratios calculated from T33, T35, and T39.

Upwelling mode	Control		Singular				Recurring			
	–	Low	Medium	High	Extreme	Low	Medium	High	Extreme	
$\Delta\text{TOC}_{\text{WC}}$ ($\mu\text{mol L}^{-1}$)	20.5	29.1	47.0	58.7	85.6	17.0	50.3	83.1	149.3	
$\Sigma\text{POC}_{\text{ST}}$ ($\mu\text{mol L}^{-1}$)	30.6	20.4	34.5	53.0	66.5	19.5	42.0	48.3	70.1	
$\Sigma\text{POC}_{\text{ST}}:\Delta\text{TOC}_{\text{WC}}$ (mol:mol)	1.49	0.70	0.73	0.90	0.78	1.15	0.84	0.58	0.47	

Data for T37 is missing because POC_{WC} was not measured on that day.

particles $> 90 \mu\text{m}$ (**Figure 4D**). The difference in porosity between particles sinking under different upwelling modes is highlighted by the visual assessment of FlowCam pictures from T11 (**Figure 4E**).

Altogether, the singular treatments exported sedimented particulate matter which was carbon- and biogenic silica-rich and sank slowly during the export event. Particles $> 100 \mu\text{m}$ were more porous compared to those in the recurring treatments. In contrast, the recurring treatments generally produced sinking particles which had lower C:N ratios, sank faster and were less porous than the ones in the singular treatments throughout the experiment.

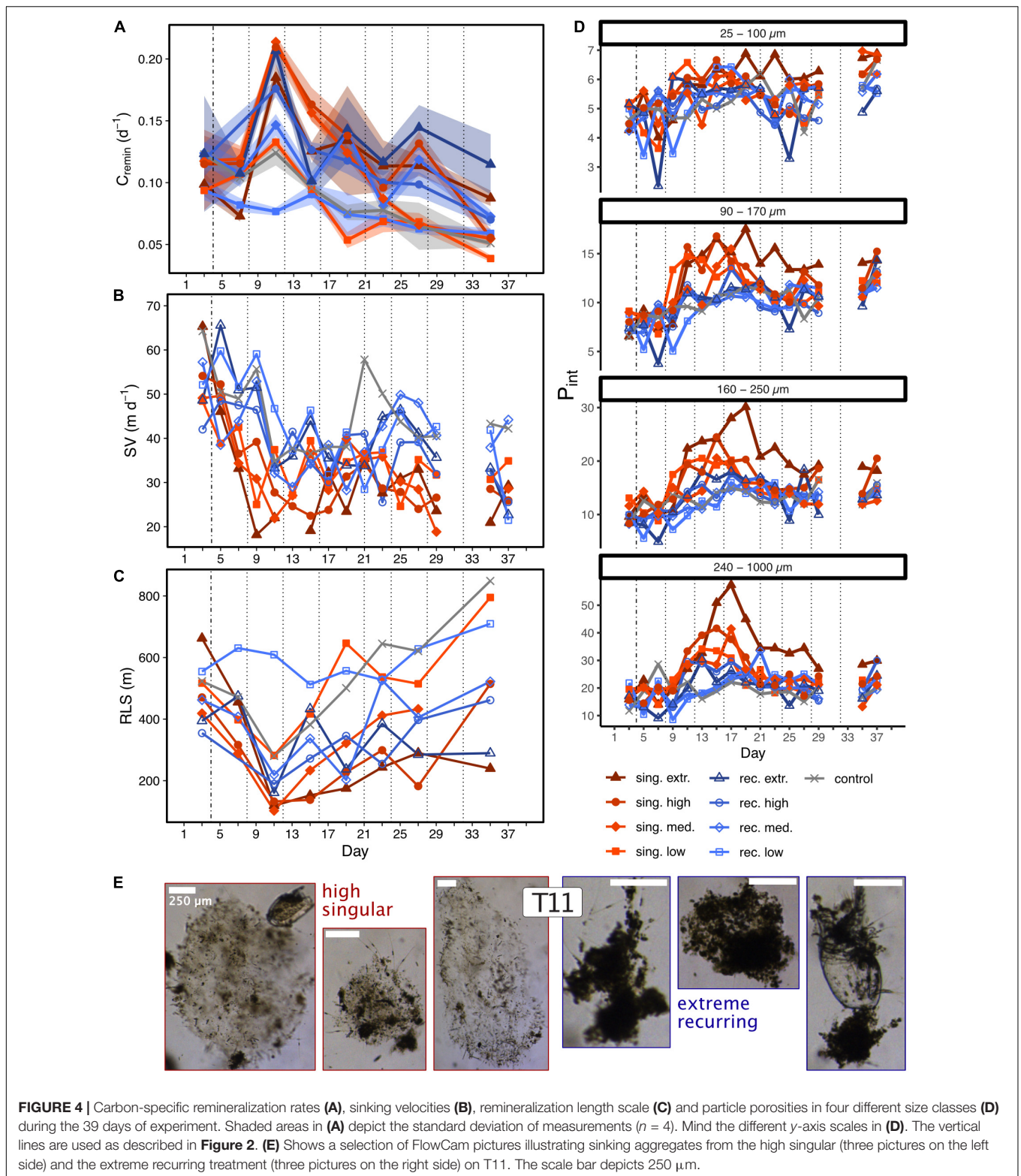
We found that upwelling intensity had significant effects on sinking particle properties and on the remineralization depth during the time we observed increased mass flux (T11–T39, **Figures 5A–C**). Particles sampled from the sediment trap sank

slowest and were remineralized most rapidly in mesocosms with high and extreme upwelling intensities. The fast remineralization rates correlated with high PHP in the water column during the same time period (**Figure 5D**). The RLS, as the quotient of SV and C_{remin} , also decreased with increasing deep water fertilization.

DISCUSSION

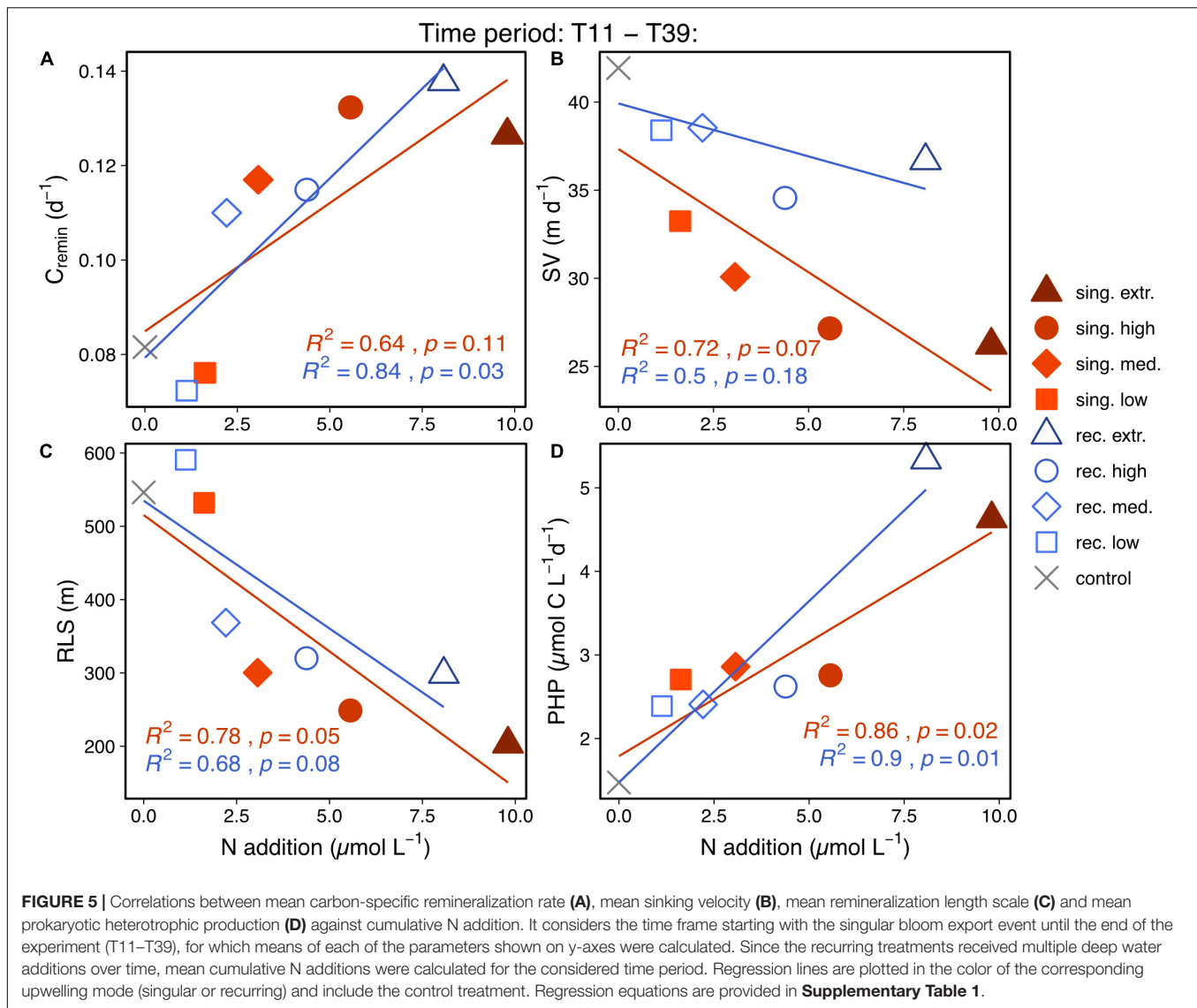
Temporal Decoupling of Biomass Production and Particulate Organic Carbon Export

We found that increased intensities of artificial upwelling resulted in higher primary productivity and POC export from the surface. However, upwelling also resulted in a temporal decoupling between biomass production ($\Delta\text{TOC}_{\text{WC}}$) and POC



export (cumulative POC_{ST}). We found that less than half of the produced organic carbon was exported in most of our upwelling treatments during our experimental duration, while the rest was retained in the water column (see Table 2). This

is consistent with findings by Taucher et al. (2017), who also fertilized Gran Canarian oligotrophic communities with a single pulse of nutrient-rich deep water, and found that roughly half of the produced particulate carbon was retained in the water



column for at least 25 days after the fertilization. Seemingly, artificial upwelling in oligotrophic surface waters does thus not lead to rapid export of most of the produced organic matter in the time scale of weeks.

Such decoupling between production and export occurs in a variety of oceanic regions (Cavan et al., 2015; Henson et al., 2019; Laws and Maiti, 2019), including eastern boundary upwelling systems (e.g., Kelly et al., 2018; Bach et al., 2020). It is thus no peculiarity of artificial upwelling. In natural upwelling systems reasons for a temporal decoupling can be e.g., persistent phytoplankton species in the water column (Bach et al., 2020) or weak trophic links in the planktonic food web (Stukel et al., 2011). A tight coupling of primary production and zooplankton consumers can generally lead to the export of high amounts of fast sinking fecal pellets, which can increase the POC export efficiency (Stukel et al., 2011; Le Moigne et al., 2016) and its transfer efficiency to depth (Steinberg and Landry, 2017). In our study, the response of the mesozooplankton community to the

deep water fertilization was not very pronounced. Although a treatment effect on mesozooplankton biomass established toward the end of the experiment, values mostly stayed on a similar or lower level compared to before the first fertilization ($\sim 20 \mu\text{g C L}^{-1}$ or lower, Spisla et al., in prep.). We also rarely observed fecal pellets in the FlowCam measurements of the sediment subsamples. The low mesozooplankton biomass and fecal pellet abundances indicate a limited impact of the mesozooplankton community on the POC flux. This hints at a potential caveat of short-term artificial upwelling as a tool for enhancing C sequestration: The fauna adapted to oligotrophic systems may not be able to readily consume great amounts of primary produced biomass and efficiently channel it into the export pathway. The dilution effect of the deep water addition amplifies the zooplankton handicap, making it even more difficult for them to catch up with the rapid phytoplankton reproduction.

Another factor that delayed the sedimentation of primary produced matter was surface microbial recycling.

Le Moigne et al. (2016) and Henson et al. (2019) found high bacterial abundances to be associated with high primary production and low export efficiency (i.e., only a small fraction of primary produced biomass is exported). Microbial recycling can channel particulate organic matter into the dissolved organic matter pool, thereby making it unavailable for metazoan consumers. Hence the breakdown of POC into DOC reduces the chances for either direct sinking of particles or incorporation and active transportation by zooplankton (Legendre and Le Fèvre, 1995). We found similar patterns of microbial activity as the above mentioned studies associated to the decoupling of primary production and export. Microbial production increased significantly with upwelling intensity in both upwelling modes (Figure 5D), thereby retaining organic matter in the surface microbial loop and making it unavailable for immediate export.

Due to the retention of organic matter in the water column, we were not able to capture the whole export response of our fertilized mesocosms, especially of the recurring highly fertilized ones. We argue that the high amounts of suspended POC (see Figure 2C) in the high and extreme recurring treatments at the end of the experiment represented a high potential for POC export, e.g., by particle aggregation and gravitational settling. Nevertheless, the retention of organic matter in the water column makes a quantitative mass flux comparison between the two upwelling modes difficult. Laws and Maiti (2019) found that the decoupling between primary and export production at the ALOHA time-series station disappears when taking into account data of monthly time intervals. We argue that the same is needed in future artificial upwelling studies. The experimental duration must be long enough to allow for the quantitative assessment of export fluxes as well as the long-term response of higher trophic levels to the enhanced surface primary production.

Upwelling Mode Shapes Sinking Particle Properties

The export events in the singular treatments were strongly linked to the preceding diatom blooms, as indicated by the elevated BSi:POC ratios in the sedimented matter (Figure 3D and Supplementary Figure 1). They featured relatively porous particles, which sank slower than the ones in the recurring treatments (Figures 4B,D), and hence resulted in a low RLS (Figure 4C). Multiple studies have shown that diatom blooms typically result in inefficient particle transfer to depth (e.g., Guidi et al., 2009; Henson et al., 2012a; Maiti et al., 2013), potentially due to the associated high particle porosities (Lam et al., 2011; Puigcorb  et al., 2015; Bach et al., 2019). Our data supports these observations, stressing the importance of a particle's porosity for its sinking velocity and thus for its potential to be transported to depth.

The influence of transparent exopolymer particles (TEP) may explain the low sinking velocities and high porosities in the singular treatments. TEP are exuded by microbial cells and facilitate the formation of aggregates (Passow, 2002; Engel et al., 2004). They can lower particle density and increase porosity, which in turn reduces particle sinking

velocity (Azetsu-Scott and Passow, 2004; Mari et al., 2017). TEP production is favored by high primary productivity and nutrient limitation (Obenosterer and Herndl, 1995), both of which occurred in the higher singular treatments on T9 (Figure 2B and Supplementary Figure 1). Additionally, the POC:PON ratio in the water column increased by > 60% from T9–T11 in the three highest singular treatments (mean values: 7.3 on T9–12.2 on T11, see Figure 4C), which indicates potentially enhanced TEP exudation. The same scenario has already been observed in a previous mesocosm experiment off Gran Canaria (Taucher et al., 2017), in which TEP concentrations were measured. During that experiment, TEP increased when the blooming phytoplankton community became nutrient limited (compare Taucher et al., 2017, 2018). We thus argue that also in our experiment increased TEP exudation was likely the cause for the reduction of particle sinking velocity in the singular upwelling mode, rendering it less efficient regarding the potential for deep POC export than the recurring mode.

Besides sinking velocity, respiration of sinking matter was another equally important factor determining the remineralization depth of sinking particles in our experiment. The temporal changes in C_{remin} were equally high (about fourfold) as the changes in sinking velocity over time. We measured the highest remineralization rates during the initial export event on T11, shortly after phytoplankton communities had shifted to diatom dominance (T7–T9, Ortiz et al., submitted). This is in accordance with earlier studies, which speculated that the structure of the phytoplankton community affects remineralization rates (e.g., Guidi et al., 2015), and have shown that diatom-dominated systems can lead to the export of sinking particles which are quickly respired (Guidi et al., 2015; Bach et al., 2019). In our case, the mechanistic reason for this could be that the particles contained a large fraction of easily degradable organic matter. We believe that the increasing porosities from T11 onward (Figure 4D) support this hypothesis. Although there are, to the best of our knowledge, no studies which found a direct positive effect of aggregate porosity on degradability, it stands to reason that higher porosities increase a particle's surface-to-volume-ratio, thus possibly enhancing its susceptibility to microbial attachment and respiration. This is in line with a hypothesis by Francois et al. (2002), who postulate that the settling of loosely packed (i.e., highly porous) aggregates leads to higher respiration rates in the mesopelagic zone. Respiration of sinking particles during this time was higher in the singular compared to the recurring treatments, likely owing to higher porosities and possibly also higher TEP concentrations. Beside the phytoplankton community structure, the zooplankton community is another factor that determines particle properties (Cavan et al., 2019). Through the packaging of phytoplankton cells into dense fecal pellets, zooplankton can make organic matter less susceptible to respiration (Steinberg and Landry, 2017). As discussed above, mesozooplankton was not abundant in our experiment, and therefore potentially not capable of repackaging the high amounts of particulate matter in the high upwelling treatments. This left the sinking biomass loosely packed for the bacterial community to feed on. We suggest that the missing repackaging of particles and the resulting high

lability of sinking organic matter was the reason for increasing remineralization with increasing upwelling intensity.

The differences in particle properties between our singular and recurring form of artificial upwelling indicate variability in the efficiency of their POC transfer to depth. Diatom spring blooms (Martin et al., 2011) and diatom communities in coastal upwelling systems (Abrantes et al., 2016) have been reported to promote efficient carbon deep export. However, the diatom blooms in our singular upwelling mode led to the export of porous, slow sinking particles, which were quickly remineralized by microbial processes. A single pulse of artificial upwelling thus resulted in a system likely to recycle the vast majority of the freshly produced organic matter in the surface ocean. Although particles in the recurring upwelling mode were respired similarly quickly, they were less porous and sank faster, which led to a slightly higher mean RLS in the recurring upwelling treatment (Figure 5C). This suggests a more efficient transfer of produced organic matter to depth under recurring upwelling conditions compared to a singular upwelling pulse.

Potential of Artificial Upwelling for Carbon Sequestration

As discussed above, one of the major factors that influence the potential of artificial upwelling for net carbon sequestration is how deep particles sink before they are remineralized (RLS). Another factor is the C:N ratio of the sinking organic matter (POC:PON), or, more generally speaking, the ratio of C to the limiting nutrient. The influence of both of these factors on carbon sequestration efficiency will be discussed in the following. We emphasize that the discussion is based upon a highly simplified 1-dimensional view of the water column, and neglects 3 dimensional movements of water masses, carbon, and nutrients through the ocean.

We start this discussion with the influence of the ratio of carbon to the limiting nutrient. Since the latter was nitrogen in our case, as is typical for large parts of the Atlantic (Moore et al., 2013), we will focus on the C:N ratio in the following. Let us assume that over long enough time scales all upwelled nutrients will be sequestered (i.e., exported to the sequestration depth), and that the upwelled deep water contains excess DIC (excess DIC = deep water DIC – surface water DIC) and excess DIN (excess DIN = deep water DIN – surface water DIN) compared to the surface ocean. In this case, a system will act as a net carbon sink if it sequesters organic matter with a C:N ratio higher than that of the upwelled excess DIC and nitrogen. In the Canary Island region, excess DIC and excess DIN between surface and 1,000 m depth (here assumed as sequestration depth) are approximately ~ 150 and $\sim 20 \mu\text{mol L}^{-1}$, respectively (Llinás et al., 1994; González-Dávila et al., 2010). This corresponds to a C:N ratio of 7.5 of upwelled excess DIC and DIN. Accordingly, for the artificial upwelling approach to generate a net carbon sink, the C:N of sequestered organic matter would need to exceed 7.5 on average, until all N added via deep water has been sequestered.

We found that artificial upwelling led to an increase in C:N ratios of sedimented matter to well above 7.5. There was

a trend of increasing POC_{ST}:PON_{ST} ratios over time in all mesocosms (Figure 3A). The ratios in the singular treatment mesocosms correlated positively with upwelling intensity in the period of highest export (T11–T21, Figure 3C). It is likely that these high ratios would have either prevailed with depth or increased even further, owing to preferential N remineralization by heterotrophic microorganisms (Boyd and Trull, 2007).

It should be noted that the control mesocosm also displayed increasing C:N ratios during the experiment. This suggests that increasing C:N might have at least partly been an enclosure effect, which also occurred in absence of an artificial upwelling treatment. By enclosing a planktonic community inside a mesocosm, the vertical mixing is reduced from the depth of the mixed layer (20–120 m in the Canary Island region, see Troupin et al., 2010) to the depth of the mesocosm (15 m in our setup). This leads e.g., to an increase of depth- and time-integrated light intensity experienced by the phytoplankton community, which may affect phytoplankton photophysiology. Moreover, the community gets truncated as large grazers (>3 mm) are excluded from the food web, thus relieving lower trophic levels like microzooplankton of grazing pressure. Both effects could have caused changes in lower trophic level productivity in our mesocosm experiment, which was fueled by leftover nutrients enclosed at experiment start (see Supplementary Figure 1), thereby leading to an increase in POC_{WC} and POC_{ST}:PON_{ST} ratios (Figures 2C, 3A). Nevertheless, the increase in sedimented matter C:N ratios was larger in those mesocosms that received deep water fertilizations, and scaled almost linearly with high upwelling rates.

Artificial upwelling can consequently enhance C:N ratios of sinking organic matter in the surface, which would favor potential carbon sequestration. This is especially the case when fertilization is carried out in single pulses. We cannot assess, however, if these ratios would have prevailed over longer time scales, i.e., until all added N had been exported with the remaining suspended particulate organic matter.

A mechanism that might counteract the positive effect of elevated C:N ratios is the observed decrease in RLS with increasing upwelling intensity in both upwelling modes. Particle sinking velocities decreased while at the same time respiration of sinking organic material accelerated with increasing nutrient input via deep water addition. Both effects resulted in a lower RLS and thus higher flux attenuation with increasing fertilization (Figures 5A–C). Earlier studies have shown that a higher fraction of export production makes it through the mesopelagic zone in less productive ecosystems and ends up in the deep ocean (e.g., Henson et al., 2012b). Our results match this finding, with less productive mesocosms showing a higher RLS than the very productive ones. These differences in RLS and thus particle transfer efficiency to depth, as well as the differences in C:N stoichiometries of sinking matter are illustrated in Figure 6.

It should be noted that our study could not assess several factors that might play an important role in determining the potential of artificial upwelling for carbon export and sequestration. First of all, our study did not account for any active biological or physical processes occurring further down the water column. Processes such as repackaging and

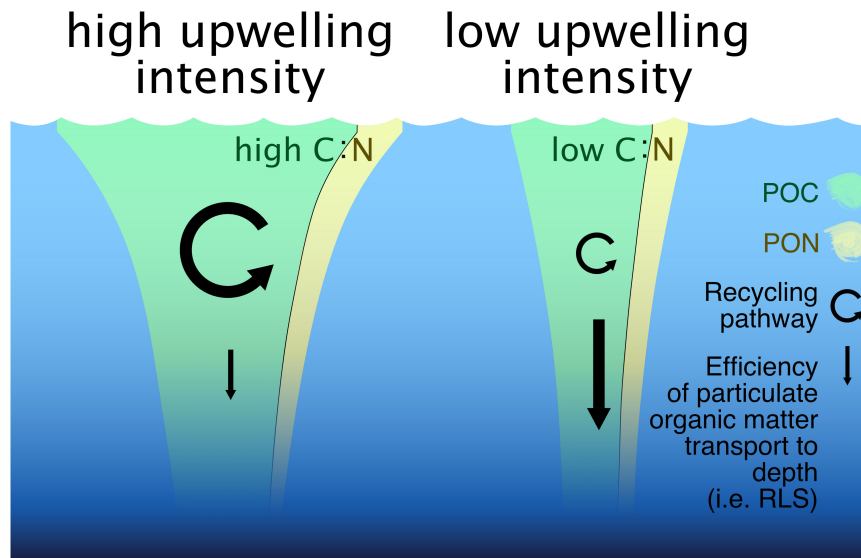


FIGURE 6 | Scheme depicting the effects that upwelling intensity had on carbon sequestration-relevant parameters in our high and low upwelling scenarios. It visualizes the strength and C:N ratio of the export flux (POC_{ST} - PON_{ST}), as well as the arrow size indicating strength of the recycling pathway and the efficiency of particle transport to depth. Note that we put more emphasis on the difference between POC:PON ratios than on the quantitative PON difference between high and low upwelling intensities. It should also be noted that the effects depicted here only reflect the initial responses to artificial upwelling in oligotrophic waters. They do not cover the ultimate fate of the upwelled inorganic nutrients and hence do not represent the long-term potential for carbon sequestration.

consumption of settling particles by zooplankton (Turner, 2015; Stukel et al., 2019) or the active diel migration of mesopelagic biota (Boyd et al., 2019 and references therein) play an important role in regulating particle transfer to depth and thus carbon sequestration (Buesseler et al., 2007; Robinson et al., 2010; Giering et al., 2014; Sanders et al., 2016; Cavan et al., 2019). Due to the limited vertical dimensions of our mesocosms, we were not able to resolve these complex processes occurring throughout the water column, and they are thus not incorporated in **Figure 6**. Secondly, due to the limited experimental duration and the decoupling between production and export of organic matter (especially in the high recurring treatments, see section “Temporal Decoupling of Biomass Production and POC Export”), we could not cover the whole export response period. We were therefore not able to draw quantitative conclusions for the carbon sequestration potential of artificial upwelling. It is likely that this potential would have increased, had the plankton communities had more time to adapt. For example, increased repackaging of suspended biomass into dense, fast-sinking fecal pellets could have favored POC deep export. Hence, we stress the need for monthly to seasonal experimental durations to validate the long-term potential of artificial upwelling for enhanced export production and carbon sequestration.

CONCLUSION AND OUTLOOK

Artificial upwelling had opposing effects on carbon export and potential transfer to the deep ocean. On the one hand, it enhanced the mass flux and C:N ratios of sinking matter. The latter is a key prerequisite for enhancing ocean carbon sequestration.

Biogeochemical modeling studies examining the feasibility of artificial upwelling in terms of carbon sequestration usually assume a static stoichiometry of C and N according to the Redfield-ratio (= 6.6). An important next step would be to re-evaluate the findings of these studies with a higher than Redfield C:N ratio as we found in our experiment. On the other hand, artificial upwelling resulted in a shallower remineralization depth and a stronger temporal decoupling between POC production and its export. The grazer community was not able to capitalize on the enhanced primary production, and hence could not form the link between biomass production and vertical flux. Thus, artificial upwelling resulted in the export of relatively porous, slowly sinking particles, which were susceptible to remineralization and therefore of low potential for deep export and sequestration. Future work should thus focus on responses of the zooplankton community and allow it more time to react to phytoplankton growth. We furthermore found that the mode, with which upwelling is applied, is an important factor for particle properties and carbon export. We found that the post-bloom export event in the singular mode produced carbon-rich particles, which were, however, respired faster and sank slower than under recurring upwelling conditions. In contrast, particle properties and the resulting RLS in the recurring mode were more favorable for POC deep export. Additionally, the continuously elevated primary and export production in the recurring mode might be more advantageous for linking the primary and export production of a slow reacting oligotrophic food web. Our assessment thus suggests that a recurring fertilization mode might be more suitable for net CO_2 removal from the atmosphere than a singular upwelling pulse. However, further research will be needed to verify if either the higher C:N ratios of sinking matter

in the singular mode or the more suitable particle properties in the recurring mode are more critical for carbon dioxide removal.

DATA AVAILABILITY STATEMENT

The datasets presented in this study can be found in an online repository. The name of the repository and accession numbers are: PANGAEA, <https://doi.pangaea.de/10.1594/PANGAEA.933090> and <https://doi.pangaea.de/10.1594/PANGAEA.933089>.

AUTHOR CONTRIBUTIONS

UR, JT, AJP, and LTB: experimental concept and design. All authors: execution of the experiment. MB, JO, MV, MH, JT, NH-H, and IB: data analysis. MB: manuscript writing with input from all co-authors.

FUNDING

This study was funded by an Advanced Grant of the European Research Council (ERC) in the framework of the Ocean Artificial Upwelling project (Ocean artUp, No. 695094). Additional Transnational Access funds were provided by the EU projects AQUACOSM (EU H2020-INFRAIA-project, No. 731065), which supported the participation of KS and MV, and TRIATLAS (EU H2020-project, No. 817578-5), which supported JA. MH received additional funding from the German Federal Ministry of Education and Research (BMBF) during this study through the PalMod Project (Nos. 01LP1505D and 01LP1919C). JA was also supported by

REFERENCES

- Abrantes, F., Cermeño, P., Lopes, C., Romero, O., Matos, L., Van Iperen, J., et al. (2016). Diatoms Si uptake capacity drives carbon export in coastal upwelling systems. *Biogeosciences* 13, 4099–4109. doi: 10.5194/bg-13-4099-2016
- Azetsu-Scott, K., and Passow, U. (2004). Ascending marine particles: significance of Transparent Exopolymer Particles (TEP) in the upper ocean. *Limnol. Oceanogr.* 49, 741–748. doi: 10.4319/lo.2004.49.3.0741
- Bach, L. T., Paul, A. J., Boxhammer, T., von der Esch, E., Graco, M., Schulz, K. G., et al. (2020). Factors controlling plankton community production, export flux, and particulate matter stoichiometry in the coastal upwelling system off Peru. *Biogeosciences* 17, 4831–4852. doi: 10.5194/bg-17-4831-2020
- Bach, L. T., Riebesell, U., Sett, S., Febiri, S., Rzepka, P., and Schulz, K. G. (2012). An approach for particle sinking velocity measurements in the 3–400 μm size range and considerations on the effect of temperature on sinking rates. *Mar. Biol.* 159, 1853–1864. doi: 10.1007/s00227-012-1945-2
- Bach, L. T., Stange, P., Taucher, J., Achterberg, E. P., Algueró-Muñiz, M., Horn, H., et al. (2019). The influence of plankton community structure on sinking velocity and remineralization rate of marine aggregates. *Global Biogeochem. Cycles* 33, 971–994. doi: 10.1029/2019GB006256
- Boxhammer, T., Bach, L. T., Czerny, J., and Riebesell, U. (2016). Technical note: sampling and processing of mesocosm sediment trap material for quantitative biogeochemical analysis. *Biogeosciences* 13, 2849–2858. doi: 10.5194/bg-13-2849-2016
- Boyd, P. W., Claustre, H., Levy, M., Siegel, D. A., and Weber, T. (2019). Multi-faceted particle pumps drive carbon sequestration in the ocean. *Nature* 568, 327–335. doi: 10.1038/s41586-019-1098-2
- Boyd, P. W., and Trull, T. W. (2007). Understanding the export of biogenic particles in oceanic waters: is there consensus? *Prog. Oceanogr.* 72, 276–312. doi: 10.1016/j.pocean.2006.10.007
- Buesseler, K. O., Antia, A. N., Chen, M., Fowler, S. W., Gardner, W. D., Gustafsson, O., et al. (2007). An assessment of the use of sediment traps for estimating upper ocean particle fluxes. *J. Mar. Res.* 65, 345–416. doi: 10.1357/002224007781567621
- Casareto, Beatriz, E., Niraula, M. P., and Yoshimi, S. (2017). Marine planktonic ecosystem dynamics in an artificial upwelling area of Japan: phytoplankton production and biomass fate. *J. Exp. Mar. Biol. Ecol.* 487, 1–10. doi: 10.1016/j.jembe.2016.11.002
- Cavan, E. L., Laurenceau-Cornec, E. C., Bressac, M., and Boyd, P. W. (2019). Exploring the ecology of the mesopelagic biological pump. *Prog. Oceanogr.* 176:102125. doi: 10.1016/j.pocean.2019.102125
- Cavan, E. L., Le Moigne, F. A. C., Poulton, A. J., Tarling, G. A., Ward, P., Daniels, C. J., et al. (2015). Attenuation of particulate organic carbon flux in the Scotia Sea, Southern Ocean, is controlled by zooplankton fecal pellets. *Geophys. Res. Lett.* 42, 821–830. doi: 10.1002/2014GL062744
- Cavan, E. L., Trimmer, M., Shelley, F., and Sanders, R. (2017). Remineralization of particulate organic carbon in an ocean oxygen minimum zone. *Nat. Commun.* 8:14847. doi: 10.1038/ncomms14847
- Cermeño, P., Fernández, A., and Marañón, E. (2012). *Determinación de La Producción Primaria Por Tamaños In Expedición de Circunnavegación Malaspina 2010: Cambio Global y Exploración de La Biodiversidad Del Océano Global: Libro Blanco de Métodos y Técnicas de Trabajo Oceanográfico*, 437–42. CSIC. Available online at: <http://hdl.handle.net/10508/4238> (accessed May 14, 2021).

a Helmholtz International Fellow Award, 2015 (Helmholtz Association, Germany).

ACKNOWLEDGMENTS

We would like to thank the Oceanic Platform of the Canary Islands (Plataforma Oceánica de Canarias, PLOCAN) for sharing their research facilities with us and for their enormous support throughout the experiment. We would also like to express our gratitude toward the Marine Science and Technology Park (Parque Científico Tecnológico Marino, PCTM), from the University of Las Palmas (Universidad de Las Palmas de Gran Canaria, ULPGC), for providing further critical research facilities. We thank the captain and crew of RV James Cook for the deployment of the mesocosms and the deep water collection, as well as the captain and crew of the vessel J.SOCAS for helping with the second deep water collection and the recovery of the mesocosms. We especially thank the KOSMOS team (GEOMAR) for taking care of the logistics and technical work necessary to conduct the mesocosm experiment. Finally, we thank Michael Sswat, Markel Gómez Letona, Carsten Spisla, Kerstin Nachtigall, Jana Meyer, Andrea Ludwig, Levka Hansen, Jannes Hoffmann, and Rokhya Bhano Kaligatla for their contribution to data analysis and data exchange.

SUPPLEMENTARY MATERIAL

The Supplementary Material for this article can be found online at: <https://www.frontiersin.org/articles/10.3389/fmars.2021.742142/full#supplementary-material>

- Engel, A., Delille, B., Jacquet, S., Riebesell, U., Rochelle-Newall, E., Terbrüggen, A., et al. (2004). Transparent exopolymer particles and dissolved organic carbon production by *emiliania huxleyi* exposed to different CO₂ concentrations: a mesocosm experiment. *Aquat. Microb. Ecol.* 34, 93–104. doi: 10.3354/ame034093
- Fan, W., Pan, Y., Zhang, D., Xu, C., Qiang, Y., and Chen, Y. (2016). Experimental study on the performance of a wave pump for artificial upwelling. *Ocean Eng.* 113, 191–200.
- Francois, R., Honjo, S., Krishfield, R., and Manganini, S. (2002). Factors controlling the flux of organic carbon to the bathypelagic zone of the ocean: factors controlling organic carbon flux. *Global Biogeochem. Cycles* 16, 34–1–34–20. doi: 10.1029/2001GB001722
- GESAMP (2019). “High level review of a wide range of proposed marine geoenvironmental techniques,” in *Rep. Stud. GESAMP No.98. IMO/FAO/UNESCO-IOC/UNIDO/WMO/IAEA/UN/UNEP/UNDP/ISA Joint Group of Experts on the Scientific Aspects of Marine Environmental Protection*, eds P. W. Boyd and C. M. G. Vivian (London: International Maritime Organization), 144.
- Giering, S. L. C., Sanders, R., Lampitt, R. S., Anderson, T. R., Tamburini, C., Boutrif, M., et al. (2014). Reconciliation of the carbon budget in the ocean’s twilight zone. *Nature* 507, 480–483. doi: 10.1038/nature13123
- Giraud, M., Boye, M., Garçon, V., Donval, A., and de la Broise, D. (2016). Simulation of an artificial upwelling using immersed in situ phytoplankton microcosms. *J. Exp. Mar. Biol. Ecol.* 475, 80–88. doi: 10.1016/j.jembe.2015.11.006
- Giraud, M., Garçon, V., De La Broise, D., L’Helguen, S., Sudre, J., and Boye, M. (2019). Potential effects of deep seawater discharge by an ocean thermal energy conversion plant on the marine microorganisms in oligotrophic waters. *Sci. Total Environ.* 693:133491. doi: 10.1016/j.scitotenv.2019.07.297
- González-Dávila, M., Santana-Casiano, J. M., Rueda, M. J., and Llinás, O. (2010). The water column distribution of carbonate system variables at the ESTOC Site from 1995 to 2004. *Biogeochemistry* 7, 3067–3081. doi: 10.5194/bg-7-3067-2010
- Guidi, L., Legendre, L., Reygondeau, G., Uitz, J., Stemann, L., and Henson, S. A. (2015). A new look at ocean carbon remineralization for estimating deepwater sequestration: ocean remineralization and sequestration. *Global Biogeochem. Cycles* 29, 1044–1059. doi: 10.1002/2014GB005063
- Guidi, L., Stemann, L., Jackson, G. A., Ibanez, F., Claustre, H., Legendre, L., et al. (2009). Effects of phytoplankton community on production, size, and export of large aggregates: a world-ocean analysis. *Limnol. Oceanogr.* 54, 1951–1963. doi: 10.4319/lo.2009.54.6.1951
- Hansen, H. P., and Koroleff, F. (1999). *Determination of Nutrients in Methods of Seawater Analysis, Third, Completely Revised and Extended Edition*, 3rd Edn. Weinheim: WILEY-VCH, 159–228.
- Henson, S. A., Sanders, R., and Madsen, E. (2012b). Global patterns in efficiency of particulate organic carbon export and transfer to the deep ocean: export and transfer efficiency. *Global Biogeochem. Cycles* 26:1028. doi: 10.1029/2011GB004099
- Henson, S. A., Lampitt, R. S., and Johns, D. (2012a). Variability in phytoplankton community structure in response to the north atlantic oscillation and implications for organic carbon flux. *Limnol. Oceanogr.* 57, 1591–1601. doi: 10.4319/lo.2012.57.6.1591
- Henson, S. A., Le Moigne, F., and Giering, S. L. C. (2019). Drivers of carbon export efficiency in the global ocean. *Global Biogeochem. Cycles* 33, 891–903. doi: 10.1029/2018GB006158
- IPCC (2018). “Summary for policymakers global warming of 1.5°C. An IPCC special report on the impacts of global warming of 1.5°C above pre-industrial levels and related global greenhouse gas emission pathways,” in *The Context of Strengthening the Global Response to the Threat of Climate Change, Sustainable Development, and Efforts to Eradicate Poverty*, eds V. Masson-Delmotte, P. Zhai, H.-O. Pörtner, D. Roberts, J. Skea, P. R. Shukla, et al. (Geneva: World Meteorological Organization)
- Iversen, M. H., and Ploug, H. (2010). Ballast minerals and the sinking carbon flux in the ocean: carbon-specific respiration rates and sinking velocity of marine snow aggregates. *Biogeochemistry* 7, 2613–2624. doi: 10.5194/bg-7-2613-2010
- Iversen, M. H., and Ploug, H. (2013). Temperature effects on carbon-specific respiration rate and sinking velocity of diatom aggregates—potential implications for deep ocean export processes. *Biogeochemistry* 10, 4073–4085. doi: 10.5194/bg-10-4073-2013
- Jakobsen, H. H., Blanda, E., Staehr, P. A., Højgård, J. K., Rayner, T. A., Pedersen, M. F., et al. (2015). Development of phytoplankton communities: implications of nutrient injections on phytoplankton composition, PH and ecosystem production. *J. Exp. Mar. Biol. Ecol.* 473, 81–89. doi: 10.1016/j.jembe.2015.08.011
- Keller, D. P., Feng, E. Y., and Oschlies, A. (2014). Potential climate engineering effectiveness and side effects during a high carbon dioxide-emission scenario. *Nat. Commun.* 5:3304. doi: 10.1038/ncomms4304
- Kelly, T. B., Goericke, R., Kahru, M., Song, H., and Stukel, M. R. (2018). CCE II: spatial and interannual variability in export efficiency and the biological pump in an eastern boundary current upwelling system with substantial lateral advection. *Deep Sea Res. 1 Oceanogr. Res. Pap.* 140, 14–25. doi: 10.1016/j.dsr.2018.08.007
- Khaliwal, S., Primeau, F., and Hall, T. (2009). Reconstruction of the history of anthropogenic CO₂ concentrations in the ocean. *Nature* 462, 346–349. doi: 10.1038/nature08526
- Khaliwal, S., Tanhua, T., Mikaloff Fletcher, S., Gerber, M., Doney, S. C., Graven, H. D., et al. (2013). Global ocean storage of anthropogenic carbon. *Biogeochemistry* 10, 2169–2191. doi: 10.5194/bg-10-2169-2013
- Kirchman, D. L., and Ducklow, H. W. (1993). “Estimating conversion factors for thymidine and leucine methods for measuring bacterial production,” in *Handbook of Methods in Aquatic Microbial Ecology*, eds P. F. Kemp, B. F. Sherr, E. B. Sherr, and J. J. Cole (Boca Raton, FL: Lewis Publishers), 513–517.
- Kwiatkowski, L., Ricke, K. L., and Caldeira, K. (2015). Atmospheric consequences of disruption of the ocean thermocline. *Environ. Res. Lett.* 10:034016. doi: 10.1088/1748-9326/10/3/034016
- Lam, P. J., Doney, S. C., and Bishop, J. K. B. (2011). The dynamic ocean biological pump: insights from a global compilation of particulate organic carbon, CaCO₃, and opal concentration profiles from the mesopelagic: the dynamic ocean biological pump. *Global Biogeochem. Cycles* 25:GB3009. doi: 10.1029/2010GB003868
- Laws, E. A., and Maiti, K. (2019). The relationship between primary production and export production in the ocean: effects of time lags and temporal variability. *Deep Sea Res. 1 Oceanogr. Res. Pap.* 148, 100–107. doi: 10.1016/j.dsr.2019.05.006
- Le Moigne, F. A. C., Henson, S. A., Cavan, E., Georges, C., Pabortsava, K., Achterberg, E. P., et al. (2016). What causes the inverse relationship between primary production and export efficiency in the southern ocean: PP and *e* ratio in the southern ocean. *Geophys. Res. Lett.* 43, 4457–4466. doi: 10.1002/2016GL068480
- Legendre, L., and Le Fèvre, J. (1995). Microbial food webs and the export of biogenic carbon in oceans. *Aquat. Microb. Ecol.* 9, 69–77. doi: 10.3354/ame009069
- Legendre, L., and Rivkin, R. B. (2002). Fluxes of carbon in the upper ocean: regulation by food-web control nodes. *Mar. Ecol. Prog. Ser.* 242, 95–109. doi: 10.3354/meps242095
- Leibold, M. A., Chase, J. M., Shurin, J. B., and Downing, A. L. (1997). *Species Turnover and the Regulation of Trophic Structure*, Palo Alto: CA Annual Reviews, 29.
- Liu, C. C. K., Dai, J. J., Lin, H., and Guo, F. (1999). Hydrodynamic performance of wave-driven artificial upwelling device. *J. Eng. Mech.* 125, 728–732.
- Llinás, O., Rodríguez de León, A., Siedler, G., and Wefer, G. (1994). *ESTOC Data Report 1994*, Las Palmas de Gran Canaria: ICCM, Dirección General de Universidades e Investigación, Consejería de Educación, Cultura y Deportes del Gobierno de Canarias, 77.
- Maiti, K., Charette, M. A., Buesseler, K. O., and Kahru, M. (2013). An inverse relationship between production and export efficiency in the southern ocean: export efficiency in the southern ocean. *Geophys. Res. Lett.* 40, 1557–1561. doi: 10.1002/grl.50219
- Mari, X., Passow, U., Migon, C., Burd, A. B., and Legendre, L. (2017). Transparent exopolymer particles: effects on carbon cycling in the ocean. *Prog. Oceanogr.* 151, 13–37. doi: 10.1016/j.pocean.2016.11.002
- Martin, P., Lampitt, R. S., Jane Perry, M., Sanders, R., Lee, C., and D’Asaro, E. (2011). Export and mesopelagic particle flux during a North Atlantic spring diatom bloom. *Deep Sea Res. 1 Oceanogr. Res. Pap.* 58, 338–349. doi: 10.1016/j.dsr.2011.01.006

- McAndrew, P. M., Björkman, K. M., Church, M. J., Morris, P. J., Jachowski, N., Williams, P. J. L. B., et al. (2007). Metabolic response of oligotrophic plankton communities to deep water nutrient enrichment. *Mar. Ecol. Prog. Ser.* 332, 63–75. doi: 10.3354/meps332063
- Moore, C. M., Mills, M. M., Arrigo, K. R., Berman-Frank, I., Bopp, L., Boyd, P. W., et al. (2013). Processes and patterns of oceanic nutrient limitation. *Nat. Geosci.* 6, 701–710. doi: 10.1038/ngeo1765
- Nielsen, E. S. (1952). The use of radio-active carbon (C14) for measuring organic production in the sea. *ICES J. Mar. Sci.* 18, 117–140. doi: 10.1093/icesjms/18.2.117
- Obernosterer, I., and Herndl, G. J. (1995). Phytoplankton extracellular release and bacterial growth: dependence on the inorganic N: P ratio. *Mar. Ecol. Prog. Ser.* 116, 247–257. doi: 10.3354/meps116247
- Oschlies, A., Pahlow, M., Yool, A., and Matear, R. J. (2010). Climate engineering by artificial ocean upwelling: channelling the Sorcerer's apprentice: ocean pipe impacts. *Geophys. Res. Lett.* 37:961. doi: 10.1029/2009GL041961
- Pan, Y., Fan, W., Huang, T.-H., Wang, S.-L., and Chen, C.-T. A. (2015). Evaluation of the sinks and sources of atmospheric CO₂ by artificial upwelling. *Sci. Total Environ.* 511, 692–702. doi: 10.1016/j.scitotenv.2014.11.060
- Pan, Y., Fan, W., Zhang, D., Chen, J. W., Huang, H., Liu, S., et al. (2016). Research progress in artificial upwelling and its potential environmental effects. *Sci. China Earth Sci.* 59, 236–248. doi: 10.1007/s11430-015-5195-2
- Passow, U. (2002). Transparent Exopolymer Particles (TEP) in aquatic environments. *Prog. Oceanogr.* 55, 287–333. doi: 10.1016/S0079-6611(02)00138-6
- Pedrosa-Pàmies, R., Conte, M. H., Weber, J. C., and Johnson, R. (2019). Hurricanes enhance labile carbon export to the deep ocean. *Geophys. Res. Lett.* 46:11. doi: 10.1029/2019GL083719
- Ploug, H., and Grossart, H.-P. (2000). Bacterial growth and grazing on diatom aggregates: respiratory carbon turnover as a function of aggregate size and sinking velocity. *Limnol. Oceanogr.* 45, 1467–1475. doi: 10.4319/lo.2000.45.7.1467
- Puigcorbè, V., Benitez-Nelson, C. R., Masqué, P., Verdeny, E., White, A. E., Popp, B. N., et al. (2015). Small phytoplankton drive high summertime carbon and nutrient export in the Gulf of California and Eastern Tropical North Pacific. *Global Biogeochem. Cycles* 29, 1309–1332. doi: 10.1002/2015GB005134
- R Core Team (2017). *R: A Language and Environment for Statistical Computing*. Vienna: R Foundation for Statistical Computing.
- Riebesell, U., Czerny, J., von Bröckel, K., Boxhammer, T., Büdenbender, J., Deckelnick, M., et al. (2013). Technical note: a mobile sea-going mesocosm system—new opportunities for ocean change research. *Biogeosciences* 10, 1835–1847. doi: 10.5194/bg-10-1835-2013
- Ristow, G. H. (1997). Wall correction factor for sinking cylinders in fluids. *Phys. Rev. E* 55, 2808–2813. doi: 10.1103/PhysRevE.55.2808
- Robinson, C., Steinberg, D. K., Anderson, T. R., Aristegui, J., Carlson, C. A., Frost, J. R., et al. (2010). Mesopelagic zone ecology and biogeochemistry—a synthesis. *Deep Sea Res. 2 Top. Stud. Oceanogr.* 57, 1504–1518. doi: 10.1016/j.dsr2.2010.02.018
- Sabine, C. L., Feely, R. A., Gruber, N., Key, R. M., Lee, K., Bullister, J. L., et al. (2004). The oceanic sink for anthropogenic CO₂. *Science* 305, 367–371.
- Sanders, R. J., Henson, S. A., Martin, A. P., Anderson, T. R., Bernardello, R., Enderlein, P., et al. (2016). Controls over Ocean Mesopelagic Interior Carbon Storage (COMICS): fieldwork, synthesis, and modeling efforts. *Front. Mar. Sci.* 3:136. doi: 10.3389/fmars.2016.00136
- Sharp, J. H. (1974). Improved analysis for 'particulate' organic carbon and nitrogen from seawater. *Limnol. Oceanogr.* 19, 984–989. doi: 10.4319/lo.1974.19.6.0984
- Smith, D. C., and Azam, F. (1992). A simple, economical method for measuring bacterial protein synthesis rates in seawater using 3H-leucine. *Marine Microbial. Food Webs* 6, 107–114.
- Stange, P., Bach, L. T., Le Moigne, F. A. C., Taucher, J., Boxhammer, T., and Riebesell, U. (2017). Quantifying the time lag between organic matter production and export in the surface ocean: implications for estimates of export efficiency: time lag and export efficiency. *Geophys. Res. Lett.* 44, 268–276. doi: 10.1002/2016GL070875
- Steinberg, D. K., and Landry, M. R. (2017). Zooplankton and the ocean carbon cycle. *Ann. Rev. Mar. Sci.* 9, 413–444. doi: 10.1146/annurev-marine-010814-015924
- Strohmeier, T., Strand, Ø., Alunno-Bruscia, M., Duinker, A., Rosland, R., Aure, J., et al. (2015). Response of *Mytilus edulis* to enhanced phytoplankton availability by controlled upwelling in an oligotrophic fjord. *Mar. Ecol. Prog. Ser.* 518, 139–152. doi: 10.3354/meps11036
- Stukel, M. R., Landry, M. R., Benitez-Nelson, C. R., and Goericke, R. (2011). Trophic cycling and carbon export relationships in the California current ecosystem. *Limnol. Oceanogr.* 56, 1866–1878. doi: 10.4319/lo.2011.56.5.1866
- Stukel, M. R., Ohman, M. D., Kelly, T. B., and Biard, T. (2019). The roles of suspension-feeding and flux-feeding zooplankton as gatekeepers of particle flux into the Mesopelagic Ocean in the Northeast Pacific. *Front. Mar. Sci.* 6:397. doi: 10.3389/fmars.2019.00397
- Svensen, C., Nejtgaard, J. C., Egge, J. K., and Wassmann, P. (2002). Pulsing versus constant supply of nutrients (N, P and Si): effect on phytoplankton, mesozooplankton and vertical flux of biogenic matter. *Sci. Mar.* 66, 189–203. doi: 10.3989/scimar.2002.66n3189
- Taucher, J., Bach, L. T., Boxhammer, T., Nauendorf, A., Achterberg, E. P., Algueró-Muñiz, M., et al. (2017). Influence of ocean acidification and deep water upwelling on oligotrophic plankton communities in the subtropical North Atlantic: insights from an in situ mesocosm study. *Front. Mar. Sci.* 4:85. doi: 10.3389/fmars.2017.00085
- Taucher, J., Boxhammer, T., Bach, L. T., Paul, A. J., Schartau, M., Stange, P., et al. (2021). Changing carbon-to-nitrogen ratios of organic-matter export under ocean acidification. *Nat. Clim. Chang.* 11, 52–57. doi: 10.1038/s41558-020-00915-5
- Taucher, J., Stange, P., Algueró-Muñiz, M., Bach, L. T., Nauendorf, A., Kolzenburg, R., et al. (2018). In situ camera observations reveal major role of zooplankton in modulating marine snow formation during an upwelling-induced plankton bloom. *Prog. Oceanogr.* 164, 75–88. doi: 10.1016/j.pocean.2018.01.004
- Troupin, C., Sangrà, P., and Aristegui, J. (2010). Seasonal variability of the oceanic upper layer and its modulation of biological cycles in the canary island region. *J. Mar. Syst.* 80, 172–183. doi: 10.1016/j.jmarsys.2009.10.007
- Turner, J. T. (2015). Zooplankton fecal pellets, marine snow, phytodetritus and the ocean's biological pump. *Prog. Oceanogr.* 130, 205–248. doi: 10.1016/j.pocean.2014.08.005
- Wickham, H., Averick, M., Bryan, J., Chang, W., D'Agostino McGowan, L., François, R., et al. (2019). Welcome to the tidyverse. *J. Open Source Softw.* 4:1686. doi: 10.21105/joss.01686
- Yool, A., Shepherd, J. G., Bryden, H. L., and Oschlies, A. (2009). Low efficiency of nutrient translocation for enhancing oceanic uptake of carbon dioxide. *J. Geophys. Res.* 114:C08009. doi: 10.1029/2008JC004792

Conflict of Interest: The authors declare that the research was conducted in the absence of any commercial or financial relationships that could be construed as a potential conflict of interest.

Publisher's Note: All claims expressed in this article are solely those of the authors and do not necessarily represent those of their affiliated organizations, or those of the publisher, the editors and the reviewers. Any product that may be evaluated in this article, or claim that may be made by its manufacturer, is not guaranteed or endorsed by the publisher.

Copyright © 2021 Baumann, Taucher, Paul, Heinemann, Vanharanta, Bach, Spilling, Ortiz, Aristegui, Hernández-Hernández, Baños and Riebesell. This is an open-access article distributed under the terms of the Creative Commons Attribution License (CC BY). The use, distribution or reproduction in other forums is permitted, provided the original author(s) and the copyright owner(s) are credited and that the original publication in this journal is cited, in accordance with accepted academic practice. No use, distribution or reproduction is permitted which does not comply with these terms.